

Finding the sources of irradiance variation at sunspot minimum

P. N. Bernasconi¹, P. Foukal², D. M. Rust¹, and B. J. LaBonte¹

¹ JHU/Applied Physics Laboratory, 11100 Johns Hopkins Road, Laurel MD 20723, USA

² Heliophysics Inc., Nahant MA 01908, USA

e-mail: pietro.bernasconi@jhuapl.edu

Abstract. In 2006-2007 the Solar Bolometric Imager (SBI) will operate in the polar stratosphere where near-space conditions can be attained for 10 to 30 days. The instrument will provide bolometric (wavelength-integrated light) and color temperature images of the Sun. At the upcoming sunspot minimum, SBI observations will be able to detect subtle sources of solar irradiance variation with the least confusion by signals from the magnetic fields. This is the best observational approach to characterizing potential causes of the long-term irradiance variations. Possible predicted sources of secular variability include torsional waves and meridional flow variations. SBI uses a 30-cm diameter F/12 Dall-Kirkham telescope with uncoated mirrors, and neutral density filters to provide broadband (bolometric) sensitivity that varies only by $\pm 7\%$ over the wavelengths from $0.31 \mu\text{m}$ to $2.6 \mu\text{m}$. Inferred solar irradiance variations will be compared with space based full-disk radiometric measurements.

Key words. Sun: activity – Sun: irradiance variation – Sun: faculae – Sun: observations

1. Introduction

Solar variability is the main external driver in climate change. Solar driving of climate may occur on timescales from decades to eons through a variety of mechanisms (reviewed by Lean 1997; Rind 2002). Heating of the troposphere by the total solar irradiance (TSI) is the most direct effect of the Sun on the Earth. A question at the research frontier is: Does luminosity variation intrinsic to the Sun drive climate change on the multi-decadal timescales relevant to the global warming problem?

Space-borne full-disk radiometry (Hickey et al. 1980; Willson et al. 1981) enables a quantitative investigation of this crucial ques-

tion. From the past two decades of radiometric observations we have learned that much of the TSI variation on solar rotational and 11-yr timescales is well correlated with surface magnetic fields such as spots, faculae, and network (Chapman & Boyden 1986; Hudson 1988; Walton et al. 2003). However, the irradiance variation on longer, multi-decadal timescales is not well characterized. The observed TSI variation over the past 25 years is small. Correlative studies overlook mechanisms that could dominate long-term variation. Furthermore, the simple monitoring of TSI variations has yielded controversial results on long-term irradiance variations (compare two methods proposed to fill the “ACRIM gap”: Fröhlich & Lean 1998; Willson & Mordinov

Send offprint requests to: P. Bernasconi

2003). An accurate description of long-term irradiance impacts on past and future climate depends on improved empirical and physical insight into TSI variation (Foukal 2003).

To gain this insight we have developed the Solar Bolometric Imager (SBI): a solar telescope equipped with an innovative bolometric detector that is capable of recording images with an angular resolution of about 5'' in essentially total photospheric light. The SBI provides the first opportunity to bolometrically image brightness variations at the solar photosphere, allowing to determine the contribution of magnetic as well as non-magnetic solar thermal structures to the TSI variation.

2. Study of Irradiance at Solar Minimum

The SBI had a first stratospheric one-day balloon flight on September 1, 2003 (Foukal et al. 2004) and in December 2006 we plan a longer flight of up to 27 days from Antarctica. Our goal is to investigate the sources of solar irradiance variation at the minimum of the solar cycle.

In the standard empirical model, all irradiance variation is caused by changes in the projected areas and contrasts of photospheric magnetic structures – sunspots, faculae, and network. This model however is incomplete, as it excludes nonmagnetic sources of irradiance variation, which may significantly contribute to the solar irradiance variability on time scales longer than the 11-yr cycle. These other sources are best studied at activity minimum, when noise from magnetic structures is least. Nonmagnetic sources include known photospheric structures such as convective cells and acoustic oscillations and inferred structures such as pole-equator temperature gradients and global variations of effective temperature.

We expect that all measurable sources of irradiance variation will have distinct spatial patterns over the solar disk, just as surface magnetic fields and convection cells have. Variation of full-disk TSI will occur from an unbalanced summation of the local contrasts. For example, the correlation of TSI with the disk-integrated

magnetic flux is nil, while the correlation with the sum of the local magnetic signals is high. Therefore, we plan to use bolometric images to understand the localized sources of irradiance variation.

During the December 2006 flight we plan to study thermal structures that span a wide temperature range, from the limb-darkening with an amplitude of 2000 K through surface magnetic fields, convection, and acoustic oscillations, to global convective and flow structures with predicted amplitudes < 1 K.

The radial temperature gradient of the photosphere produces the largest intensity signal (the limb-darkening). Limb-darkening is normally treated as a constant, but the dynamic photosphere alters its profile locally. Petro et al. (1985) modeled the range of variations expected, given changes in the source function, effective temperature, and convection in the photosphere, and showed that irradiance variations might be detectable with precise photometry. On the next flight we will achieve the kind of photometric accuracy necessary to understand the stability of limb-darkening and its correlation to TSI variation.

The extraordinary precision of TSI observations permits the detection of very weak signals from a variety of known thermal structures. For example, power spectra quickly showed 3 mHz (5-minute) acoustic oscillations at a few parts-per-million (ppm) per mode (Woodard & Hudson 1983). At lower frequencies a continuous spectrum of irradiance fluctuations is seen, identified with convective noise and active region signals (e.g. Pelletier 1996). Jimenez et al. (1999) made the correspondence between the TSI signal and the spatially resolved acoustic patterns. However, an equivalent correspondence between TSI and convective patterns does not exist. This leaves an obvious gap in characterizing irradiance variation, which we plan to fill.

Physical modeling of energy and momentum flow inside the Sun predicts several large-scale thermal structures. The highest amplitude is a pole-equator temperature difference (DeRosa et al. 2002). The existing observations are limited and do not address time variations. Helioseismic observations are beginning

to measure the form (Braun & Fan 1998) and variation (Chou & Dai 2001) of the meridional flow that is coupled to a latitudinal temperature variation. We will search for this pattern to test physical understanding of the solar interior and our techniques for probing that volume.

3. Instrument Description

The SBI consists of a 30 cm aperture F/12 Dall-Kirkham telescope feeding a 320×240 element thermal detector array. The telescope primary and secondary Pyrex mirrors are uncoated; first, to reduce the sunlight to the level suitable for the detector and second, because of the favorable reflection properties of bare Pyrex. The resulting telescope spectral transmission is flat to within $\pm 7\%$ from $0.28 \mu\text{m}$ to $2.6 \mu\text{m}$. The detector is an array of ferroelectric thermal IR elements modified by deposition of a thin coat of gold-black (Foukal & Libonate 2001; Bernasconi et al. 2004). Gold-black is a colloidal form of gold that exhibits excellent photon absorption characteristics. Its spectral absorptance vary $< 1\%$ from $0.2 \mu\text{m}$ to well beyond $3 \mu\text{m}$ (Advena et al. 1993). Incident radiation is uniformly absorbed and its energy is redistributed by the gold-black as thermal emission. The thermal emission is detected by the underlying thermal IR barium-strontium-titanate (BST) imaging array to produce an essentially flat response across all wavelengths from the UV to beyond $10 \mu\text{m}$ in the IR. For the balloon-borne SBI the spectral pass band of the detector will be between about $0.31 \mu\text{m}$ (set by the atmospheric transmission at balloon altitude) and $2.6 \mu\text{m}$ (set by the absorption of a quartz window in front of the detector array). This spectral interval contains approximately 94% of the total solar radiation.

The angular resolution of SBI is approximately $5''$, which is adequate to separate spots, faculae, and the magnetic network from non-magnetic cell interiors. SBI does not provide absolute measurements of the solar irradiance, it measures the broadband photometric contrast of localized structures, relative to their surroundings in the quiet photosphere. This measurement requires neither absolute calibration nor long term reproducibility. Because of

the relatively small size of the detector array the actual field of view of the instrument is only $917'' \times 687''$, and to obtain a full image of the Sun ($\approx 960''$ in diameter) it is necessary to create a mosaic image with the telescope pointing at 10 different locations on the solar disk. The detector frame rate is 30 Hz and 60 frames co-added, i.e., an effective integration time of 2 seconds, are sufficient to lower the noise ratio well below the solar noise induced by the Sun's 5-minute oscillations.

A five positions filter wheel is located in front of the detector. It holds two neutral density filters with attenuations factors ND1.3 and ND1.5, a step wedge filter with six attenuations ranging from ND0.7 to ND2.2, a 10 nm wide band pass filter centered at 670 nm, and a 100 nm wide band pass filter centered at 750 nm. For the bolometric observations the ND1.3 filter will be used. Such attenuation is necessary to reduce the light intensity to a level acceptable for the detector. The ND1.5 and the step wedge filters will be used for calibration purposes. Observations with the 750 nm band pass filter will provide color temperature images. Full disk mosaics recorded in-flight with the 670 nm filter will be compared with limb darkening measurements using the same filter at the McMath Solar Telescope of Kitt Peak. The comparison will help evaluating the optical response of the imager.

4. Mission Design

For the balloon-borne flight the SBI telescope is housed inside the observing platform (gondola) attached with a mount that allows to tilt the instrument in elevation. The gondola is suspended from a series of cables to the parachute and the balloon. To point the instrument at the Sun in azimuth the entire gondola is rotated around its vertical axis by means of a reaction wheel. In addition to providing pointing for the telescope the gondola houses all the electronics and mechanisms necessary to operate the instrument, to store the data and to transmit telemetry to the ground, as well as receiving commands. Power is provided by a series of photovoltaic cells. More details about the gondola and its subsystems can be found in

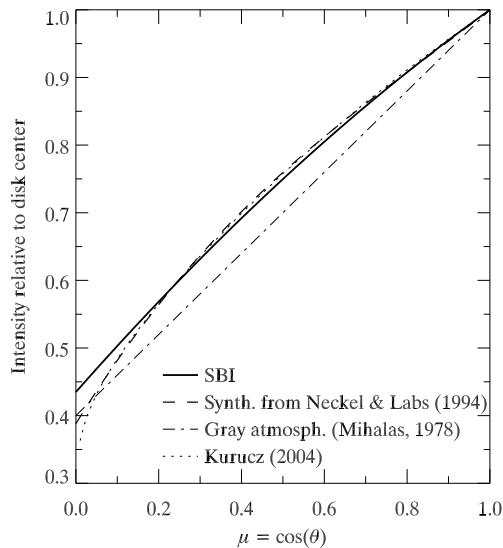


Fig. 1. Comparison of the broad-band photospheric limb-darkening function derived from the SBI observations (solid curve) with one synthesized from monochromatic data of Neckel & Labs (1994) (dashed curve), a gray atmosphere model (e.g. Mihalas 1978, dot-dashed curve), and derived from a nongray LTE atmospheric model (Kurucz 2004, dotted curve). The X-axis represents the distance from Sun center expressed in units of μ : the cosine of the angle θ between the line-of-sight and the Sun's local vertical.

Bernasconi et al. (2004) and in our web site at <http://sd-www.jhuapl.edu/SBI>.

We plan to launch the balloon borne SBI from NASA's National Scientific Ballooning Facility (NSBF) located near the McMurdo station base in Antarctica at 78 deg latitude *S*. The target launch date will be for December 2006 and the desired flight duration will be 27 days at an average altitude of 37 km. The instrument will always be in full sunlight allowing continuous observations during the entire duration of the flight. After one or two full circles around the pole the gondola will be cut from the balloon, it will safely land on the Ross Ice Shelf or the Antarctic plateau and subsequently recovered.

The basic observing program will consist of two different modes. In one mode the SBI will record series of bolometric mosaics, si-

multaneously with narrow band images with the two band pass filters. In the second mode, the telescope will stare at a fixed point, chosen for limb distance or magnetic activity, and record data at higher cadence. Observations will interleave with downlink of data samples to ensure the minimum scientific objectives. Observations will pause at intervals to acquire calibration images and recalibrate the offset pointing and the telescope focus.

Because of the relatively low telemetry data rate we will be able to download only a minimum amount of science data during the flight. Enough to guarantee our minimum science goals. The rest will be stored on-board and retrieved after landing. The on-board data storage capacity will be 1400 GB. This will allow to record SBI images compressed 50% taken at a cadence of 30 Hz for 6 hours a day for the 27 days duration of the flight.

The images will be used to derive data products such as 3D plots of intensity contrast versus $\mu = \cos(\theta)$ and magnetic flux (see Ortiz et al. 2002). The inferred TSI variation will be compared with SORCE/TIM measurements. We will make the images and data products openly available via Web access in a timely fashion.

5. Results From the First Flight of SBI

On September 1, 2003 we successfully flew the balloon-borne SBI for the first time, from a NSBF operated facility in Fort Sumner, New Mexico. The flight lasted 10 hours at an average altitude of 33 km. All the systems performed well and we captured more than 500 000 bolometric images of the Sun with a precision matched only by the non-imaging space-based radiometers. The flight provided important engineering data to validate the reliability of the gold-blackened thermal array detector, and it verified the optical and thermal performance of the SBI uncoated optics in a vacuum environment.

Here we will just briefly summarize the first scientific results from the flight. For a more detailed description and discussion see Foukal et al. (2004).

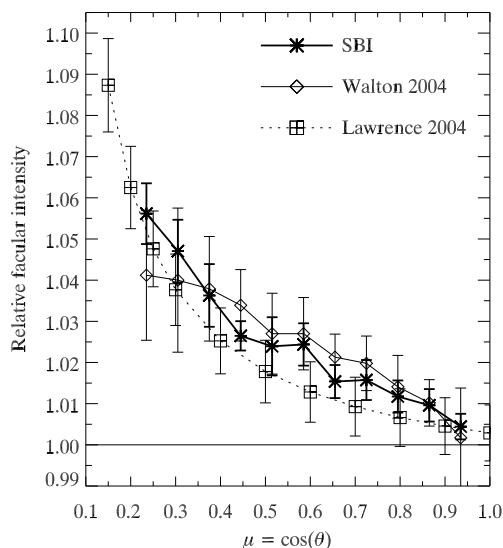


Fig. 2. Sun center-to-limb variation of the facular contrast measured by SBI in integrated light (asterisks). The curve is compared with green monochromatic measurements of Lawrence (1988) bolometrically corrected by Lawrence (2004) (squares), and with also bolometrically corrected red monochromatic measurements recorded at the San Fernando Observatory of the same faculae observed by SBI (Walton 2004) (diamonds). The vertical bars show the 1σ dispersion of the data.

5.1. Photospheric Limb-darkening

Figure 1 shows the first bolometric observation of the photospheric limb-darkening derived from a full disk mosaic taken during the SBI flight (the full disk integrated light composite that we used to derive the curve can be seen in Fig. 1 of Foukal et al. (2004)). The figure also shows a comparison with (1) a curve that we synthesized from a series of ground-based monochromatic limb-darkening measurements from Neckel & Labs (1994) and weighed by the solar flux; (2) a curve calculated from the standard formula for a gray atmosphere (e.g. Mihalas 1978); and (3) a theoretical limb-darkening function derived from a nongray LTE model atmosphere (Kurucz 2004). The SBI curve agrees to within $\pm 1\%$ with the indirect estimations of the integrated light limb darkening, with the exception of the region between $\mu = 0.15$ and the limb (corre-

sponding to about $15''$). From our analysis it is not clear whether the discrepancy near the limb is an instrumental effect or a real feature. In the next flight we will also take narrow band observations that will allow us to better test the SBI photometric response.

5.2. Facular Contrast

Figure 2 shows the center-to-limb variation intensity contrast of the bright faculae with respect to the local background intensity as observed by SBI. It was determined by sampling all the faculae within bands 0.07μ wide and then by calculating the average facular contrast in each interval. To identify and determine the position of each facula on the disk we used a CaII *K* image that was recorded at the San Fernando Observatory (SFO) when the SBI was flying. The considerable increase of the facular contrast towards the limb is a well known effect and can be explained with the hot wall facular model (see e.g. Keller et al. 2004, and references therein). However, its actual variation in integrated photospheric light was not well known, until now. The curve shown in Figure 2 is the first that has ever been derived from actual integrated light measurements.

A very interesting finding is that the SBI curve agrees remarkably well with curves obtained by applying a simple blackbody correction to a set of monochromatic measurements with angular resolution similar to that of SBI (see squares and diamonds data points in Figure 2). This suggests the interesting possibility that the integrated light contrast of faculae could be determined from existing monochromatic images of the photosphere by simply applying a blackbody correction, allowing the estimation of their contribution to the total solar irradiance.

6. Conclusions

In December 2006, at around the minimum of solar activity, we will fly the Solar Bolometric Imager on a stratospheric balloon over Antarctica for up to 27 days. The instrument will provide both integrated light (from

0.31 μm to 2.6 μm) and color temperature images of the Sun. The goal of the mission is to investigate the causes of long-term irradiance variation. The observations will allow to detect and study predicted nonmagnetic thermal structures, such as torsional waves and meridional flows, that may be the causes of secular irradiance variability. More information about the instrument and the science can be obtained by visiting our web site at: <http://sd-www.jhuapl.edu/SBI>.

Acknowledgements. We are grateful to Steve Walton for providing the SFO CaII *K* images recorded at the time SBI was flying. Special thanks for the engineering and support team at APL who designed and built the balloon borne instrument. We also thank the National Scientific Ballooning Facility for supporting the first flight of SBI. The SBI project is funded by NASA under grants NAG5-10998, and NNG05WC07G

References

- Advena D. J., Bly, V. T., & Cox, J. T. 1993, *Appl. Opt.*, 32(7), 1136
- Bernasconi, P. N., Eaton, H. A. C., Foukal, P., & Rust, D. M. 2004, *Adv. Space Res.*, 33, 1746
- Braun, D. C., & Fan, Y. 1998, *ApJ*, 508, L105
- Chapman, G. A., & Boyden, J. E. 1986, *ApJ*, 302, L71
- Chou, D.-Y., & Dai, D.-C. 2001, *ApJ*, 559, L175
- DeRosa, M. L., Gilman, P. A., & Toomre, J. 2002, *ApJ*, 581, 1356
- Foukal, P. 2003, *EOS*, 84, 205
- Foukal, P., & Libonate, S. 2001, *Appl. Opt.*, 40, 1138
- Foukal, P., Bernasconi, P. N., Eaton, H. A. C., & Rust, D. M. 2004, *ApJ*, 611, L57
- Fröhlich, C., & Lean, J. *Geophys. Res. Lett.*, 25, 4377
- Hickey, J. R., Stowe, L. L., Jacobowitz, H., Pellegrino, P., Maschhoff, R. H., House, F., & Vonder Haar, T. H. 1980, *Science*, 208, 281
- Hudson, H. S. 1988, *ARA&A*, 26, 473
- Jimenez, A., Roca Cortes, T., Severino, G., & Marmolino, C. 1999, *ApJ*, 525, 1042
- Keller, C. U., Schüssler, M., Vögler, A., & Zakharov, V. 2004, *ApJ*, 607, L59
- Kurucz, R. L. 2004, private communication
- Lean, J. 1997, *A&A*, 35, 33
- Lawrence, J. K. 1988, *Sol. Phys.*, 116, 17
- Lawrence, J. K. 2004, private communications
- Mihalas, D. 1978, *Stellar Atmospheres*, 2nd ed., Freeman
- Neckel, H., & Labs, D. 1994, *Sol. Phys.*, 153, 91
- Ortiz, A., Solanki, S. K., Domingo, V., Fligge, M., & Sanahuja, B. 2002, *A&A*, 388, 1036
- Pelletier, J. D. 1996, *ApJ*, 463, L41
- Petro, L. D., Foukal, P. V., & Kurucz, R. L. 1985, *Sol. Phys.*, 98, 23
- Rind, D. T. 2002, *Science*, 296, 673
- Walton, S. R. 2004, private communications
- Walton, S. R., Preminger, D. G., & Chapman, G. A. 2003, *ApJ*, 590, 1088
- Willson, R. C., Gulkis, S., Janssen, M., Hudson, H. S., & Chapman, G. A. 1981, *Science*, 211, 700
- Willson, R. C., & Mordvinov, A. V. 2003, *Geophys. Res. Lett.*, 30, 1199
- Woodard, M., & Hudson, H. 1983, *Sol. Phys.*, 82, 67